Cellulose conversion to lactic acid over supported HPAs catalysts

Asimina A. Marianou[a,b], Chrysoula C. Michailof[*,a], Dimitrios Ipsakis[a], Konstantinos Triantafyllidis[*,b], Angelos A. Lappas[a]

Supporting Information

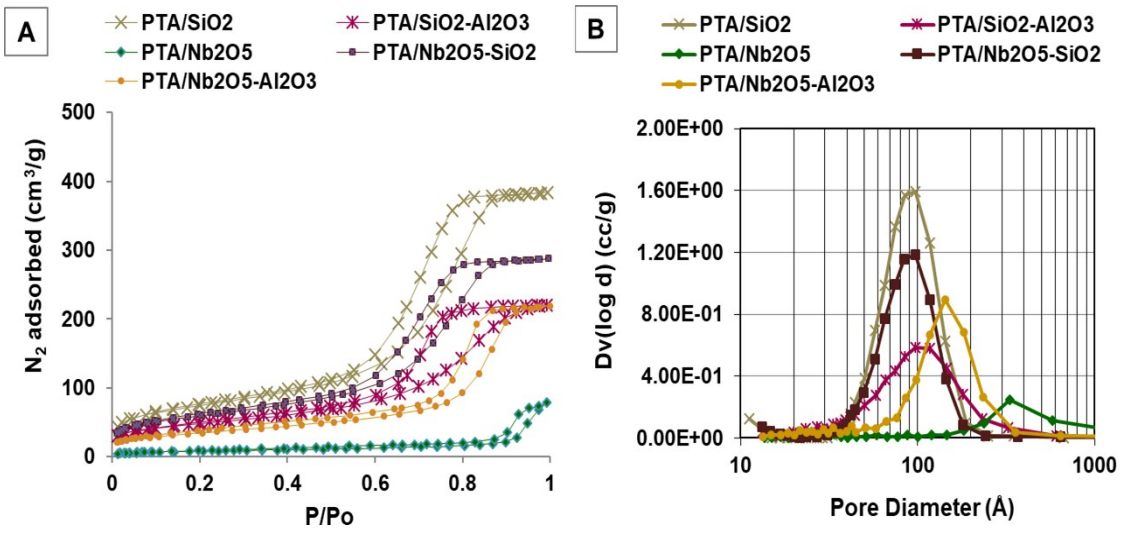

Figure S1: (A) N_2 adsorption-desorption isotherms and **(B)** respective pore size distribution curves (based on BJH analysis of adsorption data) of PTA supported catalysts.

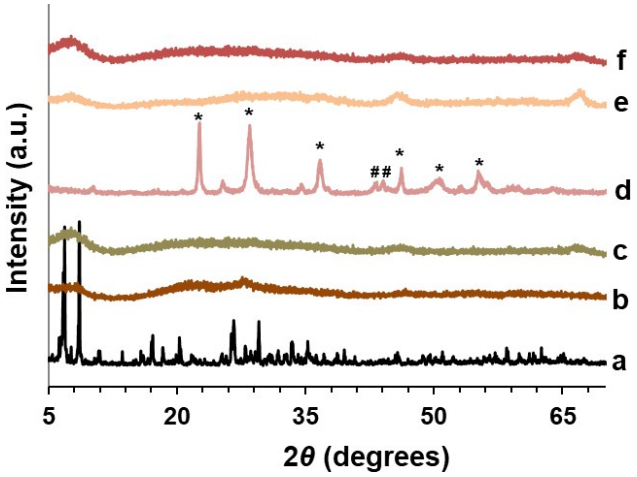

Figure S2: XRD patterns of PTA supported catalysts: **a)** PTA ($H_3PW_{12}O_{40}$), **b)** PTA/SiO_2, **c)** PTA/SiO_2-Al_2O_3, **d)** PTA/Nb_2O_5: (*) orthorhombic (T) and (#) monoclinic (M and H) phases of Nb_2O_5, **e)** PTA/Nb_2O_5-Al_2O_3, **f)** PTA/Nb_2O_5-SiO_2.

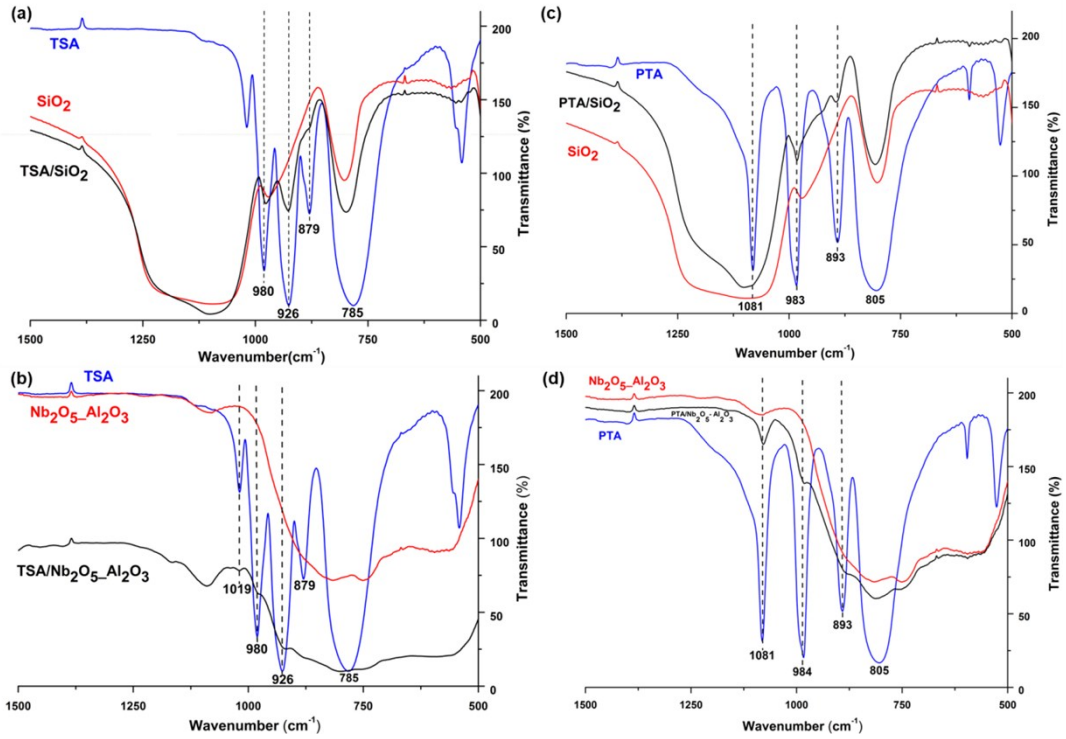

Figure S3: FT-IR spectra of pure TSA ($H_4SiW_{12}O_{40}$), pure PTA ($H_3PW_{12}O_{40}$), **(a)** SiO_2, TSA/SiO_2, **(b)** Nb_2O_5-Al_2O_3, TSA/Nb_2O_5-Al_2O_3, **(c)** SiO_2, PTA/SiO_2 and **(d)** Nb_2O_5-Al_2O_3, PTA/Nb_2O_5-Al_2O_3.

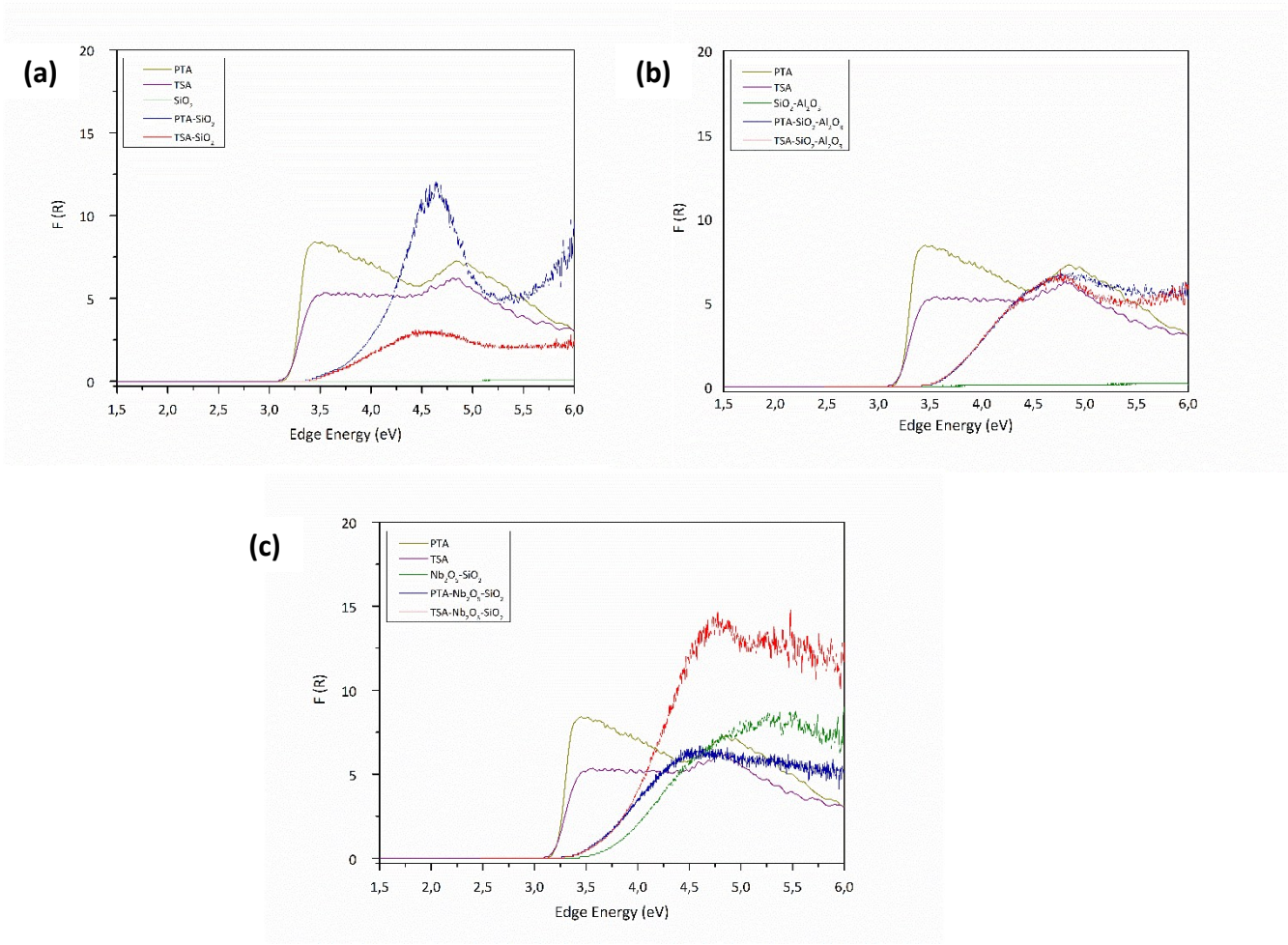

Figure S4: Diffuse-reflectance UV-Vis spectra of pure TSA ($H_4SiW_{12}O_{40}$), pure PTA ($H_3PW_{12}O_{40}$), **(a)** SiO_2, TSA/SiO_2, PTA/SiO_2, **(b)** SiO_2-Al_2O_3, TSA/SiO_2-Al_2O_3, PTA/SiO_2-Al_2O_3 and **(c)** Nb_2O_5-SiO_2, TSA/Nb_2O_5-SiO_2, PTA/Nb_2O_5-SiO_2.

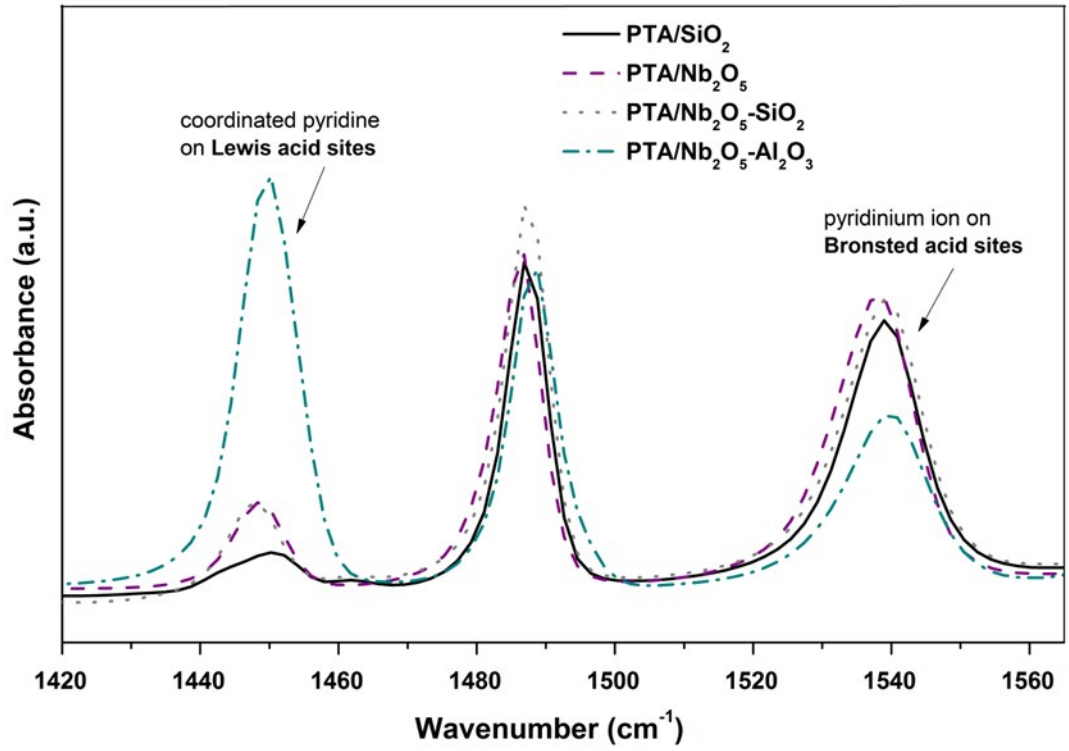

Figure S5: FT-IR/sorbed pyridine spectra of the PTA supported catalysts.

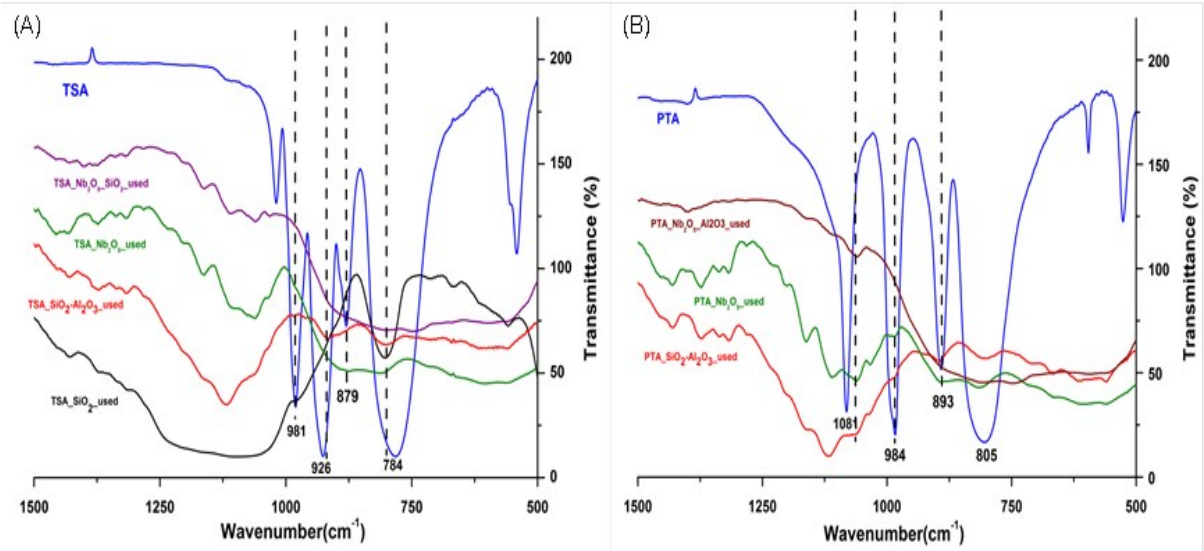

Figure S6: FT-IR spectra of:

(A) pure TSA ($H_4SiW_{12}O_{40}$) and TSA/SiO_2, TSA/SiO_2-Al_2O_3, TSA/Nb_2O_5, TSA/Nb_2O_5-SiO_2 used dried catalysts after the reaction and

(B) pure PTA ($H_3PW_{12}O_{40}$) and PTA/SiO_2-Al_2O_3, PTA/Nb_2O_5, PTA/Nb_2O_5-Al_2O_3 used dried catalysts after the reaction

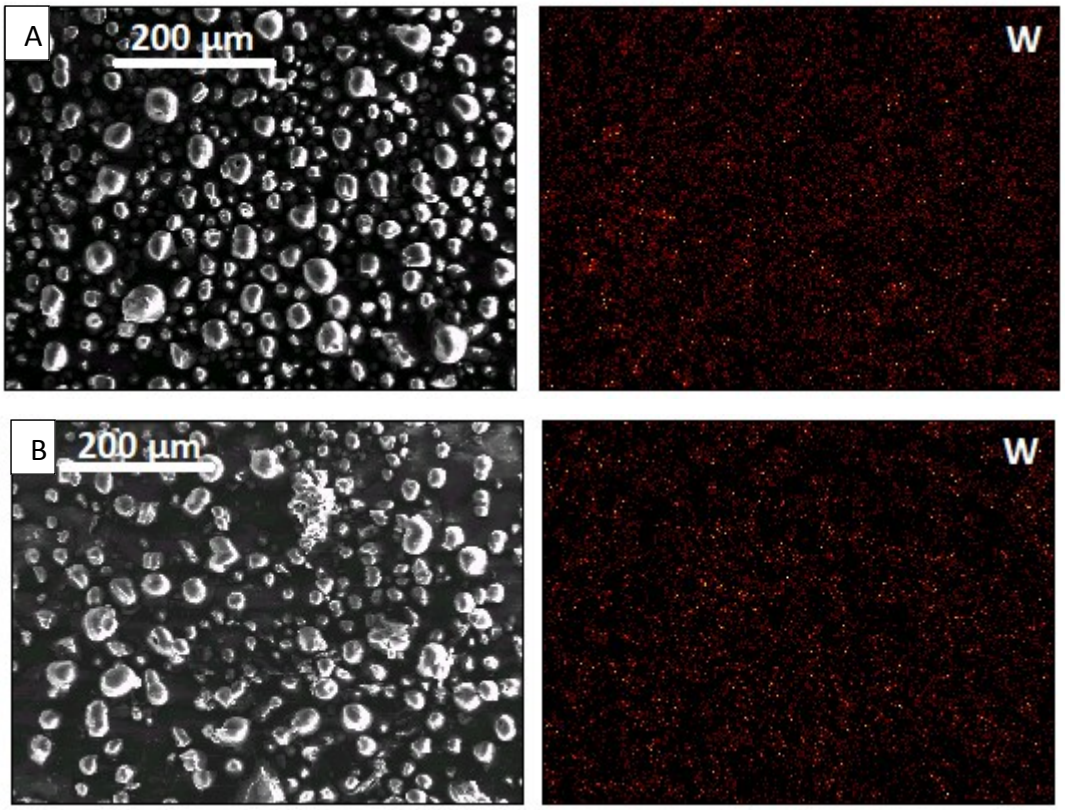

Figure S7: SEM-EDS elemental mapping of W for TSA/SiO_2-Al_2O_3 **(A)** fresh and **(B)** used calcined sample.

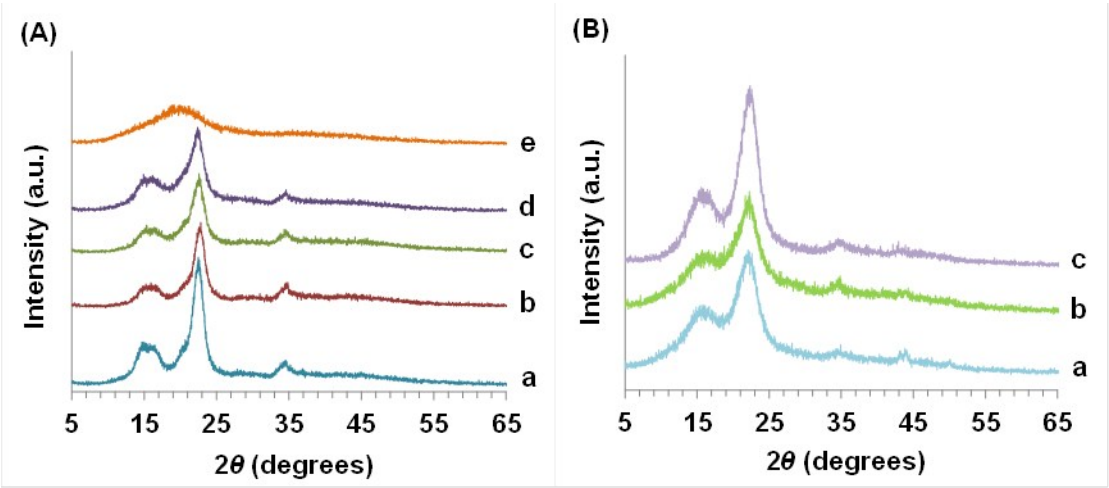

Figure S8: XRD patterns of **(A)** microcrystalline and treated cellulose: **(a)** MCC, **(b)** son.cel_2h, **(c)** son.cel_4h, **(d)** b.m.cel._10h, **(e)** b.m.cel._24h and **(B)** different kind of biomass **(a)** Lignocel, **(b)** Lig.hem.free, **(c)** del.Lig..

Reaction Kinetics

The postulated kinetic scheme of cellulose conversion towards lactic acid is presented in Scheme 2 of the main text. In order to verify the initially stated assumptions of the 5 overall reaction stages, a set of experiments was performed. In each set, only the reactant (starting material) was varied in order to

kinetically evaluate its conversion towards the various products. Through this strategy, the reversibility of each reaction could easily be validated both experimentally and theoretically, while the prominent reaction pathways towards the main components could be understood and kinetically modeled. **Table S1** postulates each experimental set and the main objective (related to the kinetic scheme) in each set. All kinetic experiments were performed at isothermal conditions (T=175 ^{o} C, t= 90 min) for the best performing TSA/SiO_2-Al_2O_3 catalyst, in aqueous medium and in the absence of mass/heat transfer limitations (kinetically controlled regime). The latter have been ensured by conducting all experiments in low catalyst weights, high concentration of reactants and continuous stirring. In this way, external and internal limitations can be excluded.

Table S1: Set of experiments conducted during kinetic modeling investigation (Feed: 6 wt. %, Catalyst: 6 wt. %, T= 175 ^{o}C, t= 90 min).

Starting Material	Cellulose	Glucose	Fructose	HMF	Lactic Acid
Kinetically evaluate the formation of:	Glucose, Fructose, HMF, Lactic acid, Organic acids*	Fructose, HMF, Lactic acid, Organic acids*	Glucose, HMF, Lactic acid, Organic Acids*	Formic acid, Levulinic acid, Humins	Formic acid

**Organic acids: Glycolic Acid, Formic Acid, Levulinic Acid*

A power law kinetic scheme was developed and applied towards evaluating the proposed reaction **Scheme 2**, following an nth order kinetic modeling approach with regards to the main reactant. The corresponding equations **1-9** are shown in **Table S2.**

Table S2: Kinetic modeling equations and estimated parameters.

Equation	parameters	A/A
$\frac{d[Cellulose]}{dt} = -k_1 \cdot [Cellulose]^{n_1}$	k_1=0.047 n_1=1.93	**(1)**
$\frac{d[Glu\cos e]}{dt} = k_1 \cdot [Cellulose]^{n_1} - k_{+2a} \cdot [Glu\cos e]^{n_{2a}} - k_{2b} \cdot [Glu\cos e]^{n_2} + k_{-2a} \cdot [Fructose]^{n_{3a}}$	k_{+2a}=0.401 k_{-2a}=0.583 n_{2a}=1.47	**(2)**
$\frac{d[Glycolic\ Acid]}{dt} = k_{2b} \cdot [Glu\cos e]^{n_2}$	k_{2b}=0.438 n_2=1.54	**(3)**
$\frac{d[Fructose]}{dt} = k_{+2a} \cdot [Glu\cos e]^{n_2} - k_{-2a} \cdot [Fructose]^{n_{3a}} - (k_{3a} + k_{3b} + k_{3c}) \cdot [Fructose]^{n_3}$	k_{3a}=0.470 k_{3b}=0.778 k_{3c}=0.221 n_{3a}=1.72	**(4)**
$\frac{d[Lactic\ Acid]}{dt} = k_{3b} \cdot [Fructose]^{n_3}$	n_3=1.32	**(5)**
$\frac{d[HMF]}{dt} = k_{3a} \cdot [Fructose]^{n_3} - (k_{4a} + k_{4b}) \cdot [HMF]^{n_4}$	k_{4a}=0.040 k_{4b}=0.118 n_4=1.41	**(6)**
$\frac{d[Formic\ Acid]}{dt} = k_{4a} \cdot [HMF]^{n_4} + k_{3c} \cdot [Fructose]^{n_3}$		**(7)**

$$\frac{d[Levulinic\ Acid]}{dt} = k_{4a} \cdot [HMF]^{n_4} \quad \textbf{(8)}$$

$$\frac{d[Hu\min s]}{dt} = k_{4b} \cdot [HMF]^{n_4} \quad \textbf{(9)}$$

[Component] denotes the respective component molar mass in mol, t the total run time in min, k_i the kinetic constant of i_{th} reaction in $1/min \cdot mol^{nj}$ and n_i the empirical reaction order in i_{th} reaction.

The 1st order ordinary differential equations **(1)-(9)** were solved under the 4th order Runge Kutta method, whereas the optimal estimation of the kinetic parameters k_i /n_i was performed under a nonlinear constraint optimization problem that leads to the minimization of the squared error between experimental (Y_{exp}) and simulated (Y_{sim}) values:

$$\min F_{obj} = \sum_{i}^{n} (Y_{\exp} - Y_{sim})_i^2 \ .$$

The estimated kinetic parameters are shown in **Table S2.**

Based on individual experiments conducted with the lactic acid as a starting material, it was verified that under the imposed reaction conditions and the specific catalyst TSA/SiO_2-Al_2O_3, lactic acid is not decomposed or reacted in a worth mentioning rate. Only after 24 h a mere 10 % conversion was calculated, which is clearly insignificant. Hence, lactic acid is considered as a stable product in this kinetic study and the reaction route towards acidic products is excluded (**Scheme 2**). **Figures S9a-h** compare the kinetic modeling results (simulation) with the experimental data for all sets shown in **Table S1** above. As it is clearly seen, the proposed reaction scheme along with the related kinetic modeling equations predicts successfully the evolution profiles of all components irrespective of the starting material. Both glucose and fructose are reaching conversions of ~100 % after 90 min (**Figures S9 a and b)** and that is the main reason of choosing such a low reaction time for the kinetic modeling investigation. The overall reaction rate of fructose is significantly higher than that of glucose proving that the selected catalyst TSA/SiO_2-Al_2O_3 is more selective towards fructose conversion. As it is further observed, lactic acid **(Figure S9d)** is produced in a higher rate when fructose is in a higher concentration, which highlights the importance of glucose isomerization towards fructose (main reactant towards lactic acid). HMF evolution profile **(Figure S9c)** also shows a slightly higher rate when fructose is used as a starting material, which further justifies the higher rate of formic and levulinic acids formation **(Figures S9 e and f)**. Clearly, when HMF is the starting material the conversion of the HMF towards formic and levulinic acid is significantly higher, but as already mentioned, this is a function, solely of its initial concentration and not a catalytic effect. Regarding the individual formation of formic acid from fructose as shown in **Scheme 2**, **Figure S9h** shows the evolution profile of this component when fructose and glucose are used as starting materials. As was expected, formic acid formation is higher when fructose is used in a higher concentration and especially during the first 20 min. A rather interesting result is reported for glycolic acid (**Figure S9g)**, where a significantly higher rate is reported when glucose is used as a starting material. This further verifies the proposed kinetic **Scheme 2**, where glycolic acid is formed only through glucose. This is actually the reason for the (overall) slower formation rate of glycolic acid when fructose is used as a starting material since a significant period of time is required for the isomerization of fructose to glucose and then to glycolic acid (the reaction scheme goes backwards from fructose to glucose and then to glycolic acid).

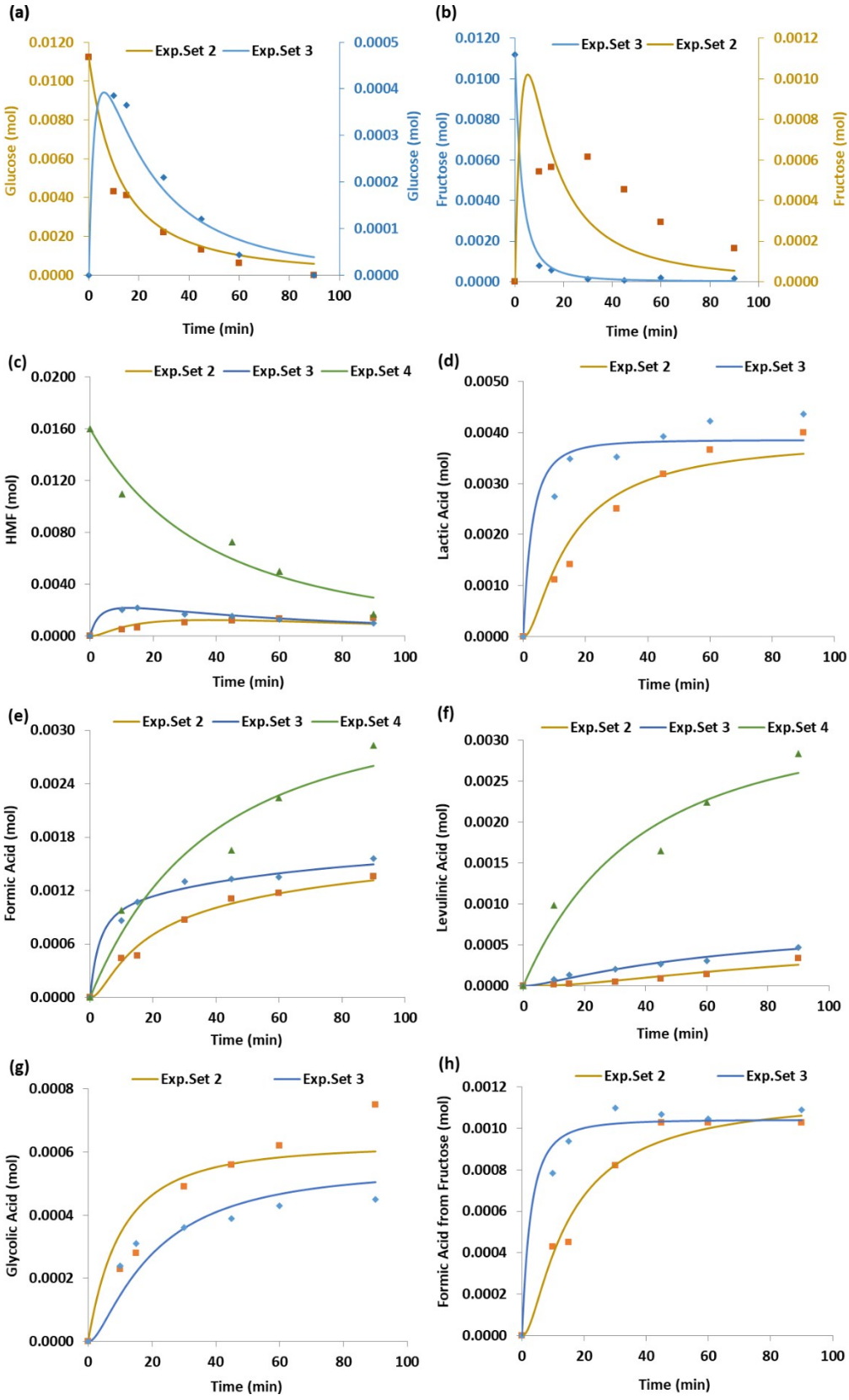

Figure S9: Comparison between experimental (symbol) and simulated (line) results for **(a)** glucose **(b)** fructose, **(c)** HMF, **(d)** lactic acid, **(e)** formic acid, **(f)** levulinic acid, **(g)** glycolic acid and **(h)** formic acid

from fructose, under isothermal reaction conditions in the presence of TSA/SiO_2-Al_2O_3 (**Exp. Set 2**: feed = glucose**, Exp. Set 3**: feed = fructose, **Exp. Set 4**: feed = HMF).
Based on the above analysis, a long-term experiment featuring cellulose as a starting material was performed. In this way, the suitability of the proposed kinetic modeling scheme could be further verified and theoretically validated. In contrast with the previous reaction times of t=90 min, the optimal reaction time of 48 h was selected in order to estimate only the kinetic parameters k_1, n_1 and validate the rest from the previous analysis. As shown in **Figures S10a-d**, the kinetic modeling results predict satisfactorily the experimental profiles of the respective components. Since the experiment was performed in prolonged run times, intermediate components such as HMF, fructose and glucose were in a very low amount and not shown explicitly. Thus, the components profiles have been grouped in lactic acid (main product), glycolic acid (to represent its individual formation from glucose) and total acids (formic and levulinic). As was expected, lactic acid is the main product of cellulose degradation followed by the total formic and levulinic acids.

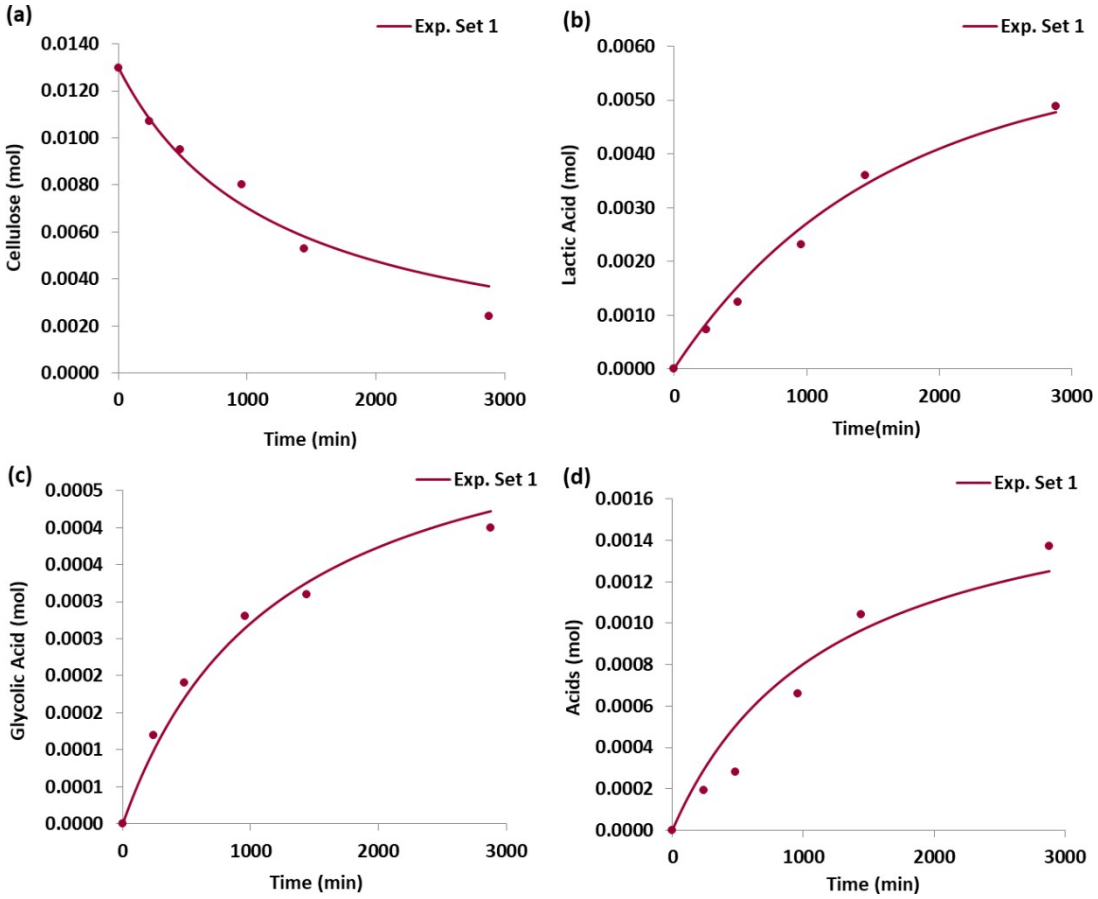

Figure S10: Comparison between experimental (symbol) and simulated (line) results for **(a)** cellulose, **(b)** lactic acid, **(c)** glycolic acid and **(d)** total acids (levulinic and formic acid) with cellulose as a starting material (Exp. Set 1), under isothermal reaction conditions in the presence of TSA/SiO_2-Al_2O_3.

The above results can be quantified (up to a reasonable extent) by the kinetic parameters of **Table S2**. Specifically, the values of k_{3a}, k_{3b} and k_{3c} denote the ranking of the production of lactic acid > HMF > formic acid from fructose. Similarly, the production of humins from HMF is performed at a higher rate as compared to the respective rate of formic and levulinic acid formation from HMF (k_{4b}>k_{4a}). Finally, the reversible reaction of glucose from/to fructose is performed under a similar rate (very close values of k_{+2a}, k_{-2a} and n_{2a}, n_{3a}).
Overall, the kinetic investigation proved that the proposed reaction scheme (**Scheme 2**) follows a power law kinetic modeling approach. All experimental data were recorded under the same reaction conditions, but with different starting materials, and were accurately predicted by the kinetic modeling set under minor deviations. For the latter, the parity plots (**Figure S11**) and the summarized statistical

analysis (**Table S2**) are provided for clarification. Clearly, such an analysis aids on the identification of prominent reaction routes, as well as, provides insights on the formation rates of various components.

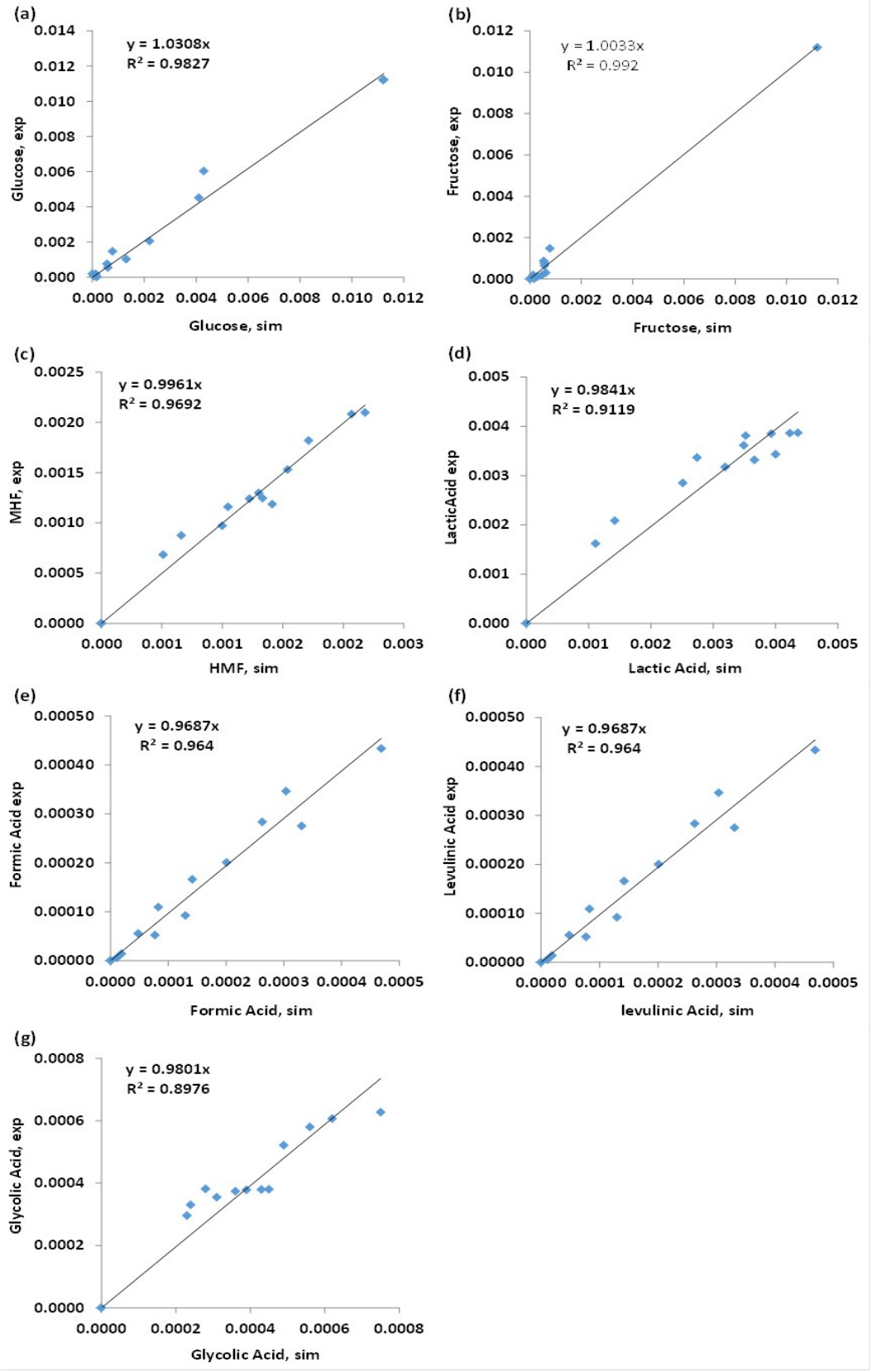

Figure S11: Parity plots denoting the accuracy of the kinetic modeling results for: **(a)** glucose, **(b)** fructose, **(c)** HMF, **(d)** lactic acid, **(e)** formic acid, **(f)** Levulinic acid, **(g)** glycolic acid.

Table S2. Overall statistic evaluations.

Sq.Error	R^2	Rel. Error
5.3E-4	0.94	10-15%

Sq.Error: Sum of squared error between experimental and simulated values (the objective function in section 3.6), **R^2:** r-squared, **Rel. Error:** Relative absolute error between experimental and simulated values